J Mol Model (2011) 17:2525–2538
DOI 10.1007/s00894-010-0915-1

ORIGINAL PAPER

Homology model and docking studies on porcine β_2 adrenoceptor: description of two binding sites

Marvin A. Soriano-Ursúa · José Correa-Basurto · José G. Trujillo-Ferrara · Alberto J. Kaumann

Received: 27 July 2010 / Accepted: 22 November 2010 / Published online: 4 January 2011

Abstract The affinity of the classical β_2 adrenoceptor-selective inverse agonist ICI118,551 is notoriously lower for porcine β_2 adrenoceptors ($p_2\beta$AR) than for human β_2 adrenoceptors ($h\beta_2$AR) but molecular mechanisms for this difference are still unclear. Homology 3-D models of $p\beta_2$AR can be useful in predicting similarities and differences, which might in turn increase the comparative understanding of ligand interactions with the $h\beta_2$AR. In this work, the $p\beta_2$AR amino acid sequence was used to carry out homology modeling. The selected $p\beta_2$AR 3-D structure was structurally and energetically optimized and used as a model for further theoretical study. The homology model of $p\beta_2$AR has a 3-D structure very similar to the crystal structures of recently studied $h\beta_2$AR. This was also corroborated by sequence identity, RMSD, Ramachandran map, TM-score and *docking* results. Upon performing molecular *docking* simulations with the AutoDock4.0.1 program on $p\beta_2$AR, it was found that a set of well-known β_2AR ligands reach two distinct binding sites on $p\beta_2$AR. Whereas one of these sites is similar to that reported on the $h\beta_2$AR crystal structure, the other can explain some important experimental observations. Additionally, the theoretical affinity estimated for ICI118,551 closely agrees with affinities estimated from experimental in vitro data. The experimental differences between the human/porcine β_2ARs in relation to ligand affinity can in part be elucidated by observations in this molecular modeling study.

Keywords β_2 adrenoceptor · Flex-ligand docking · GPCR · Homology modeling · Pig · 7TM receptors

Electronic supplementary material The online version of this article (doi:10.1007/s00894-010-0915-1) contains supplementary material, which is available to authorized users.

M. A. Soriano-Ursúa · J. Correa-Basurto · J. G. Trujillo-Ferrara
Departments of Physiology, Biochemistry and Molecular Modeling. Escuela Superior de Medicina,
Instituto Politécnico Nacional,
Plan de San Luis y Díaz Mirón,
11340 Mexico City, Mexico

A. J. Kaumann
Department of Physiology, Development and Neuroscience,
University of Cambridge,
Downing Street, Physiology Building, Cambridge,
Cambridge CB2 3EG, UK

M. A. Soriano-Ursúa (✉)
Departamento de Fisiología y Farmacología,
Escuela Superior de Medicina,
Plan de San Luis y Díaz Mirón,
Mexico City, D.F. 11340, Mexico
e-mail: msoriano@ipn.mx

Introduction

The β_2 adrenoceptor (β_2AR) is a major target receptor for drug development. Several drugs targeted for β_2AR, are used for the treatment of some respiratory and other diseases in humans [1]. β_2AR agonists have also been applied to promote muscle growth and to limit lipid deposition in livestock [1, 2].

The understanding of the human β_2AR ($h\beta_2$AR), which was the second seven-transmembrane domain receptor (7TM) characterized by X-ray methods [3–5], has helped to develop the knowledge of 7TM ligand recognition and receptor activation [6, 7]. Based on the crystallography structures, molecular modeling studies have yielded robust 3-D models for the analysis of ligand interaction with the β_2AR [8–11].

β_2AR ligands are commonly tested on animal models and recombinant receptors. In some species such as guinea pigs, the potencies and efficacies of agonists and antagonists on the β_2AR are similar to those on hβ_2AR, which has been observed both in vitro [12] and in silico experiments [13]. This similarity in affinity appears to be due to 3-D structural characteristics shared by the β_2ARs of these two species [13]. Additionally, it is known that the amino acids of β_2AR (and other 7TMs) are conserved at the binding site in the majority of species investigated so far [13–16]. However, different affinity values for some ligands, including β_2AR-selective ICI118,551, have been reported for hβ_2AR compared to some other species, such as frog and pig [17, 18]. Since the molecular mechanisms for these differences are still unclear, homology 3-D models of pβ_2AR can be useful for predicting key-punctual residues, conformational states and different binding sites, which might in turn increase the comparative understanding of ligand interactions with the hβ_2AR [19]. The comparison of the porcine and human structural β_2-adrenoceptor components that determine the affinity for ICI118,551 could provide rational starting points for the synthesis of chemical leads towards new receptor-selective ligands.

In the present study, homology modeling was used to build the pβ_2AR and well-known ligands were docked on it in order to clarify the specific interactions involved and to infer affinity for the complex formed. The results were compared with previously reported experimental data about structural differences between ligand interactions with pβ_2AR and hβ_2AR.

Methods

pβ_2AR 3-D model building

The NCBI protein sequence data base [http://www.ncbi.nlm.nih.gov/sites/entrez] was used to search the sequence of amino acids for pβ_2AR. The employed sequence was reported by Liang [20] et al. (ID: NP_001121908; 418 amino acids). The BLAST server [http://blast.ncbi.nlm.nih.gov] was used to align the pβ_2AR sequence with the hβ_2AR template amino acids sequences (Identity=84.0 %, Suppl. Fig. 1). Homology modeling of pβ_2AR was then carried out using the automated form of I-Tasser [21–23], Swiss-model [24–26] and PS^2 [27]. All servers used as template the crystal structure of hβ_2AR reported by Rasmussen [3, 28] et al. (PDB code: 2r4r) or the structure reported by Cherezov [4] et al. (PDB code: 2rh1). The obtained models were evaluated by means their RMSD, TM-score [29], 3-D visualization by comparison with the crystal structure (model 2rh1 without T4-lysozyme) and their Ramachandran plots obtained by Rampage server (Table S1) [30].

Receptor refinement

The selected pβ_2AR model was refined in vacuo during 10000 steps at 0 K using the steepest descendent protocol employing the CHARMM27 parameters implemented in the NAnoscale Molecular Dynamics (NAMD 2.6) program [31]. This straightforward procedure has improved the β_2AR 3-D structure without disrupting the ligand binding site [13, 19]. The refined pβ_2AR model was analyzed by 3-D superimposition on its template, the TM-align program [32] and Ramachandran plot.

Ligands retrieval

A set of 46 structures of β_2AR-ligands (full, partial and inverse agonists and antagonists) was used to determine the binding energy and binding modes on the refined pβ_2AR model (Fig. 1), including a compound reported as an hβ_2AR agonist by our group [33]. For each ligand, except for catechol and dopamine, the R and S-enantiomeric structures were built from their 3-D (or 2-D) structures which were downloaded from the Drug Bank database [http://www.drugbank.ca/drugs]. Only the β (to amine) carbon was considered as chiral center, except for ICI118,551 (Fig. 1), which was analyzed in its four stereoisomer forms (see below). The 3-D structures of the ligands were geometrically optimized at the B3LYP/6-31G (d,p) level using Gaussian 98 [34].

Methodology for ligand-receptor recognition study

To identify the pβ_2AR recognition site and determine the ligands' affinities for this receptor, *docking* simulations were performed using 3-D ligand/receptor structures. To corroborate availability of the putative binding site in the selected and refined models, a binding site prediction was carried out by using Q-site Finder program [35].

Docking methodology

All rigid/flexible bonds, partial atomic charges (Gasteiger-Marsili formalism), and non-merge hydrogen of the ligands were assigned. The Kollman partial charges for all atoms in the hβ_2AR/pβ_2AR, its solvatation parameters, and the non-merged hydrogens were added using AutoDock Tools 1.5.0 while maintaining the other program's default parameters [36]. *Docking* simulation were performed using a commonly-used search algorithm (hybrid Lamarckian Genetic) implemented in AutoDock 4.0.1 [36]. The initial population was 100 randomly placed individuals, and the

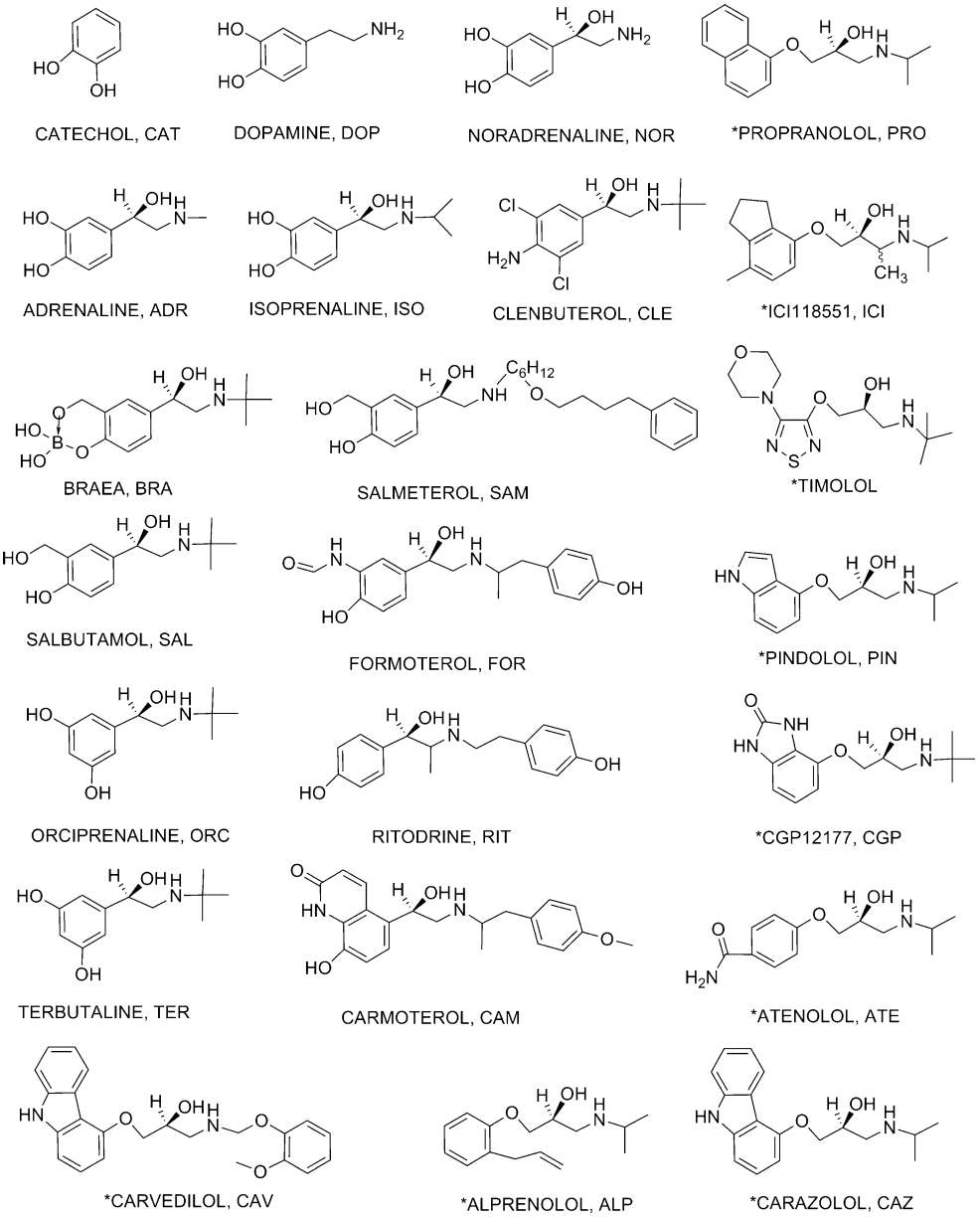

Fig. 1 Ligands tested on the porcine β_2AR model, asterisk is in ligands with antagonist or inverse agonist activity. Chiral centers depicted in this scheme were considered for building 3-D ligand representations. Hence, at least two isomeric forms for the majority of ligands were used

maximum number of energy evaluations was 10 million. To avoid interaction on inaccessible surfaces (lipid bilayer membrane and intracellular), the input initializations of the ligand structures and hβ_2AR/pβ_2AR-binding-site were defined by using a GRID-based procedure [36] making a 80×80×80 Å point grid with 0.375-Å spacing was used, centered at Cα of Asp113 [37]. Docked orientations within a root mean square deviation (RMSD) of 0.5 Å were clustered together. The lowest free-energy cluster returned for each compound was used for further analysis using Autodock Tools 1.5.0. Docking results (pβ_2AR-ligand complexes) were visualized and analyzed by using VMD 1.8.6 [38]. Additionally, theoretical docking assays with flexible lateral chains of some amino acids in TM5 (Tyr 199, Ser203, Ser204 and Ser207) were carried out because this procedure has been reported to improve the affinity estimation and also could contribute to fit agonist or antagonist into the binding site [39].

Comparison between in silico simulations and in vitro assays on pβ_2AR

The AutoDock tools 1.5.0 was used to obtain the intermolecular affinity values (free energy, ΔG and pK_d) for the ligand-pβ_2AR complexes with lowest free-energy (highest affinity) [36]. These results were compared with the affinity values of well-known ligands on the pβ_2AR reported from in vitro assays on recombinant pβ_2AR [18].

Results and discussion

Homology modeling

Eight 3-D models for pβ_2AR (Table S1) were obtained by homology modeling with three different servers. Model 1 from the I-Tasser server was selected due to its great 3-D similarity to crystal structures according to its RMSD, TM-score and the C-score. This model contains all 418 amino acids of the pβ_2AR sequence and no omissions or mistakes were observed in visualization of the superimposition with the hβ_2AR crystal structure (Fig. 2). The extra five amino acids found in the cloned pβ_2AR [20] that do not exist in hβ_2AR were included in the carboxyl intracellular fragment.

The refined pβ_2AR model has a RMSD slightly higher than that for the unrefined form due to deviation in the backbone of intracellular and second extracellular loops (Fig. 2, Table S1). However, the structure of the pβ_2AR and hβ_2AR are very similar in both cases, and the TM domains and obviously the main binding site were conserved. The Ramachandran plot for refined pβ_2AR shows amino acids in the disallowed region (Suppl. Fig. 2) are in loops, except for Asn322, which is included in TM6.

The binding sites on the pβ_2AR

Binding site prediction from servers

The I-Tasser server provided an initial binding site prediction on the selected model derived from a consensus of the top five functional homologues taken from crystal structures found in the Protein Data Bank. Additionally, the Q-site finder server identified ten sites in each structure, of which only three sites in the selected model (Suppl. Fig. 3) and two sites in the refined pβ_2AR structure were in dimensional and viable position for ligand recognition based on the known data for β_2AR activation. The predicted sites in the refined structure are depicted in Fig. 3. The volume reported by the Q-site finder (in cubic Å units) was 744 for site 1 and 464 for site 2 of pβ_2AR. Two similar sites were found in the hβ_2AR crystal structure (PDB code: 2rh1), with a volume of 877 for site 1 and 367 for site 2. The smaller volume in the hβ_2AR model for site 2 could cause restricted access to ligands, probably explaining why site 2 was not found in previously reported *docking* simulations on the β_2AR at the lowest ligand-receptor energy values (see Fig. 3) [6, 8, 9, 40, 41].

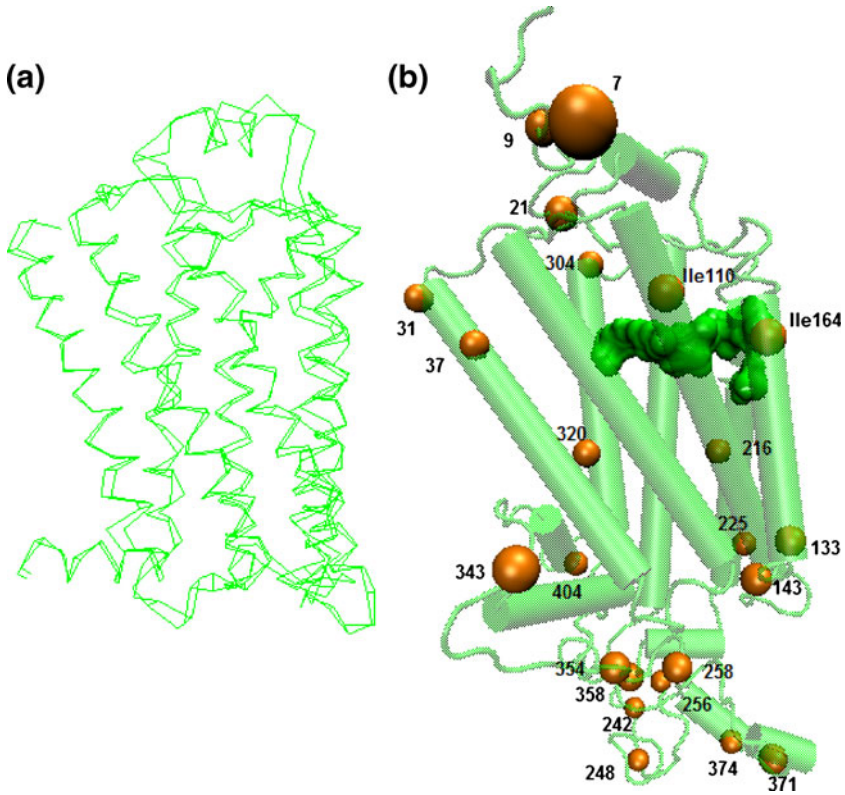

Fig. 2 Comparison between human and porcine β_2AR. (**a**) 3-D alignment of common residues between β_2ARs from TM-Align program. (**b**) A pβ_2AR model showing (in orange beads) the different amino acids between species. The amino acids Ile110 and Ile164 are located near the main binding site (some amino acids in this site -Asp113, Asn312, Ser204 and Ser207- are in the green surface representation)

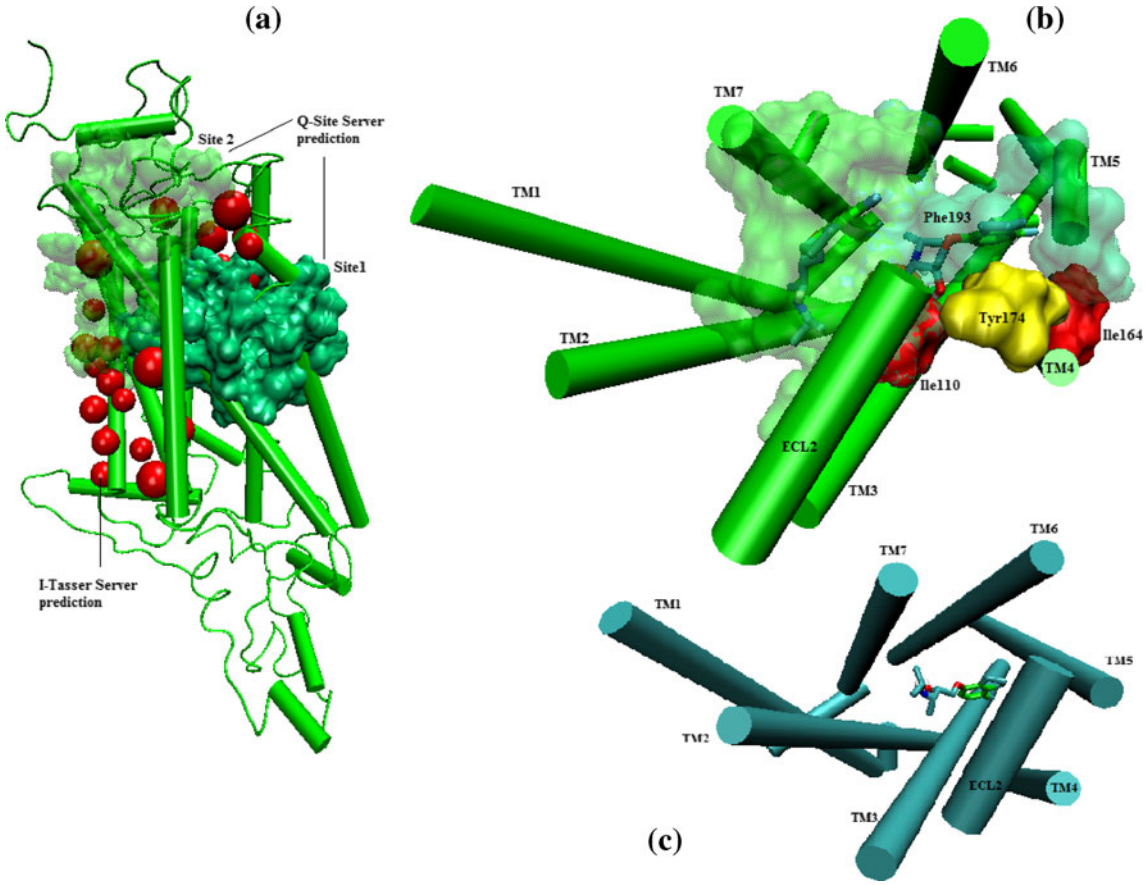

Fig. 3 Binding sites predicted on the pβ_2AR. (**a**) By servers: Q-site predicted sites are in surface representation, volume for site 1 is 744 Å^3 and 464 Å^3 for site 2. I-Tasser server-predicted residues are in beads representation. (**b**) Predicted sites viewed in *docking* simulations for S,S-ICI118551; the amino acids which interactions were found in these complexes are in diminished surface. Additionally, amino acids that differ from amino acids in the hβ_2AR are in red and Tyr174 which is not in the binding site of the hβ_2AR is in yellow. (**c**) The binding site for S,S-ICI118551 on the hβ_2AR (estimated by same methodology as for pβ_2AR)

Ligand binding sites found by docking simulations on the pβ_2AR model

Experimental and theoretical studies with β_2AR have revealed that some residues play an essential role in ligand binding (Table 1). These residues or their homologues were considered as the 'main binding pocket' (as named by Nygaard et al. [42]) in the hβ_2AR and pβ_2AR 3-D models. Whereas this site showed similar dimensions and spatial distribution (Site 1, Fig. 3) in both models, two amino acids are different near this site in the two species, and they are considered essential for ligand binding: in the positions where Ile110 and Ile164 are found in pβ_2AR (Fig. 3b), threonines exist in wild type hβ_2AR. Thr110 has already been suggested as a key residue in hβ_2AR activation according to previous theoretical simulations [15] and for Thr164, cell expression assays for hβ_2AR-Ile164 showed disruption in ligand binding and functional properties. Moreover, Thr164Ile coincides with an uncommon hβ_2AR polymorphism, which has been related to changes of affinity of certain ligands [43, 44].

Tyr174 in the pβ_2AR model is located at the top of the binding pocket together with Phe193 (Fig. 3) in accordance with the suggestion that Tyr174 is an essential part of the binding pocket for the hβ_2AR in relation to the interaction of partial agonists, according to molecular dynamic simulations [45]. In the hβ_2AR crystal structure this residue is located toward the extracellular face of the receptor, meaning that it may be implicated in ligand-specific regulation at the receptor surface [46].

Unexpectedly, a second binding site (not previously reported) was determined for the majority of ligands included in the *docking* simulations on the rigid-pβ_2AR. At this site, which coincides with what I-Tasser and Q-

Table 1 Amino acids implicated in the ligand binding site for hβ_2AR and comparison with the pβ_2AR model

Ballesteros- Weinstein position	Suggested important by theoretical/ experimental data in hβ_2AR[a]	Amino acids in pβ_2AR[b]	With ligand contacts on pβ_2AR model[c]	
			Site1	Site 2
2.57	Val86	Val86		XD
2.67	Met 96	Met 96		
3.28	**Trp109**	Trp109	**d**	**Xd**
3.29	**Thr110**	**Ile110**	**D**	**X**
3.32	**Asp113**	Asp113	**XD**	**XD**
3.33	**Val 114**	Val 114	**Xd**	**Xd**
3.36	**Val 117**	Val 117	**X**	**XD**
3.37	**Thr118**	Thr118	**XD**	
4.56	~~Thr164~~	**Ile164**	Xd	Xd*
4.57	~~Ser165~~	Ser165		Xd*
4.60	Pro168	Pro168		X*
ECL2.33	Tyr174	Tyr174	XD	
ECL2.49	Cys190	Cys190		
ECL2.50	Cys191	Cys191		X*
ECL2.51	Asp192	Asp192		XD*
ECL2.52	**Phe193**	Phe193	**D**	**XD***
ECL2.54	**Thr195**	Thr195	**D**	**X**
5.35	Asn196	Asn196		
5.38	**Tyr199**	Tyr199	**D**	
5.39	**Ala200**	Ala200	**D**	
5.42	**Ser203**	Ser203	**XD**	
5.43	**Ser204**	Ser204	**D**	
5.46	**Ser207**	Ser207	**XD**	
5.47	Phe208	Phe208	XD	
6.44	Phe282	Phe282	X	
6.48	**Trp286**	Trp286	**XD**	
6.51	**Phe289**	Phe289	**XD**	**D**
6.52	**Phe290**	Phe290	**XD**	
6.55	**Asn293**	Asn293	**D**	
7.35	**Tyr308**	Tyr308		**XD***
7.39	**Ans312**	Ans312	**XD**	**XD**
7.42	Gly315	Gly315	X	
7.43	**Tyr316**	Tyr316	**X**	**XD**

[a] From Fatakia et al. [15], except the crossed out which were included due to experimental studies by Green [43] et al. and Chelikani [57] et al. suggesting a key role. In bold the amino acids for which there is ligand contact in crystal structure; the amino acids considered key in the theoretical study of reference are underlined

[b] The amino acids different to hβ_2AR are in bold

[c] Amino acids which form binding sites; from the Q-site finder server (X) and from docking simulations (D if the amino acid is consistent between ligands and **d** if not). In bold amino acids which have ligand contact in crystal structure. Asterisks are in amino acids in site 2 for which exists experimental evidence of ligand affinity disruption [42, 57, 58]

site finder servers predicted as a potential interaction surface, there are amino acids which belong to TM2, TM3, TM4, TM7, and some that are included in the second extracellular loop. Some amino acids located in TM3 and TM7 are shared in site 2 and site 1 of the β_2AR (Table 1).

The two binding sites on the rigid pβ_2AR model and their relation with experimental observations of β_2AR ligand recognition

As observed with human β_1AR, two different agonist affinity values have been measured in binding assays on

recombinant $p\beta_2AR$, or functionally with $h\beta_2AR$ (see Fig. 3), leading to the hypothesis that there are two binding sites, and/or two or more conformational states in the ligand-β_2AR interaction. Evidence exists that supports each of these possibilities. For instance, experimental studies using fluorescent or bioluminescent resonance energy transfer support the latter idea, and that the particular conformation of the receptor is influenced by ligand-binding [47]. Also experimentally, ligand saturation analysis supports the existence of two distinct binding sites for several ligands with agonist properties on $p\beta_2AR$ [18]. The possible co-existence of two binding sites and two or more conformations was also proposed for β_1AR [48].

Some computational studies support the existence of different 7TM conformational states, which is consistent with the different signaling found experimentally [42, 49–54]. Furthermore, it is accepted that 7TMs can support a wide variety of ligand-binding modes that have differing degrees of interaction with regions involved in known conformational switches. Thus, the capacity to generate conformationally adequate models from crystal structures taking ligand-induced states into account is an important topic [8, 9].

On the other hand, theoretical studies with rigid 7TMs-crystal or refined structures have been carried out to reproduce experimental data [8, 15, 33, 40]. One of the first *docking* simulations on the β_2AR crystal was reported by Audet and Bouvier [41], in which specific subsets of amino acids were found in the shared recognition site for different ligands. They suggested an association between the recognition subsets and the ligand activity on the Gs or/and mitogen-activated protein kinase (MAPK) [55].

In the present study, we found not only a subset of amino acids for specific ligands, but also provide the first theoretical evidence of two distinct binding sites on β_2ARs, which was suggested by the Q-site finder server and corresponds to ligand conformations with the highest ligand-β_2AR affinity values by *docking* simulations (see Fig. 3).

In the $h\beta_2AR$ and turkey-β_1AR crystal structures, homologous binding sites have been observed and share some residues in conserved positions with the A_{2A} adenosine receptor [15, 56]. In our simulations two binding sites for ligands in $h\beta_2AR$ crystal structures were also found, but only one was homologous with those previously reported, and the majority of agonists (R and S forms) showed the highest affinity for this homologous site. Peculiarly, R/S-terbutaline and S-carmoterol did not interact with Asp113 in the highest affinity conformation (as reported with inverse agonists for adenylyl cyclase and MAPK by Audet and Bouvier) [41], but instead with Val86 in TM2 or Trp109 in TM3, and with Tyr306 and Asn312 in TM7.

Whereas most amino acids in TM3 and TM7 are shared by both sites found in our $p\beta_2AR$ model, there are some amino acids found in site 2 that are not in site 1 (Table 1): Val86 in TM2, Trp109 in TM3, Ser165 in TM4 (suggested by the Q-site finder server only), as well as Cys191 and Asp192 in ECL2. Additionally, none of the amino acids included in TM5 in site 1 are in site 2.

Mutational studies of the $h\beta_2AR$ have shown disruption in ligand binding for some residues in site 2 (specifically Thr164, Ser165, Pro168, Cys191, Cys192, Phe193 and Tyr308, see Table 1). Also, some studies have demonstrated the role of Ser165, Cys190 and Cys191 which are residues in a highly conserved group in β_2AR- in stabilizing ECL2 [57, 58]. Mutagenesis β_2AR studies that could support an important role for any other of the amino acids identified in site 2 are still pending. Moreover, the disposition of most ligands in site 2 seems to be like that of the phenol ethylamine moiety of ZM241385 in the respective binding site of the A_{2A} adenosine receptor (Fig. 4) [42]. The greatest similarity in the binding conformation of ZM241385 on the A_{2A} adenosine receptor and that of salmeterol on $p\beta_2AR$ was in terms of the type of residues involved in affinity with the respective ligands. In fact, S-salmeterol showed only one binding site in these docking studies, but this molecule had interactions with residues implicated in both binding sites in this conformation (Fig. 4b).

Theoretical ligand affinity values from the modeled $p\beta_2AR$ and their relationship with experimental observations on $p\beta_2AR$

We explored the correlation between some reported experimental pk_d values [18] and the predicted theoretical values determined for agonist or antagonist.

The high-affinity values for agonists (considering salbutamol and clenbuterol as outliers) on the rigid model of $p\beta_2AR$ coincide with site 1. In this sense, it is possible to observe some correlation with high state experimental values. However, the predicted affinity values were lower than the corresponding affinity values experimentally determined for high-affinity-site, but greater than those reported for the low-affinity site values.

For the antagonists propranolol and ICI118,551 the affinity prediction was similar to experimental values, suggesting a close relationship of our $p\beta_2AR$ model to the putatively inactive state, as in the $h\beta_2AR$ crystallized forms with inverse agonist and antagonists [6, 7, 41, 59]. However, whether or not the state of 7TMs is active or inactive remains unclear, though some works have improved the understanding of this question [39, 50]. With our $p\beta_2AR$ model there is correlation between a set of experimental and theoretical values, both for agonists and

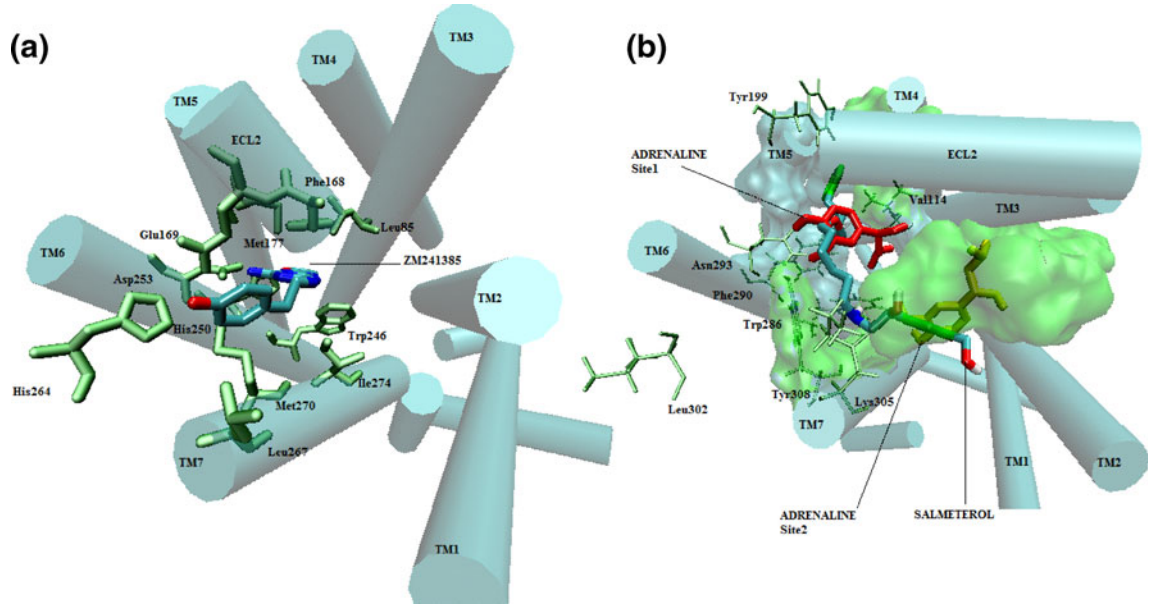

Fig. 4 Similitude of the site 2 on $p\beta_2AR$ with the site observed in A_{2A} adenosine receptor. (**a**) A_{2A} adenosine receptor with ZM241385 in its binding site. Amino acids in the binding site are in bonds. (**b**) Binding site of adrenaline and salmeterol on our $p\beta_2AR$ model. Homologues amino acids to the A_{2A} adenosine receptor in the $p\beta_2AR$ are depicted in bonds, and the amino acids which correspond to site 1 (blue) and site 2 (green) are in surface representation

antagonists (R^2=0.8853; Fig. 5, Suppl. Fig. 5), as determined with equation 1:

$$\text{Experimental } pK_d \approx \text{Corrected } pK_d \text{ value} = 1.2771(pK_d \text{ calculated}) - 1.0692) \quad (1)$$

Equation 1 seems therefore to be adequate for estimating experimental affinity from theoretical data (see hyphens and filled rhombs in Fig. 5).

The use of flexible lateral chains of residues in TM5 did not improve the affinity prediction on the $p\beta_2AR$ model employed in the current study in relation to most ligands. The affinity

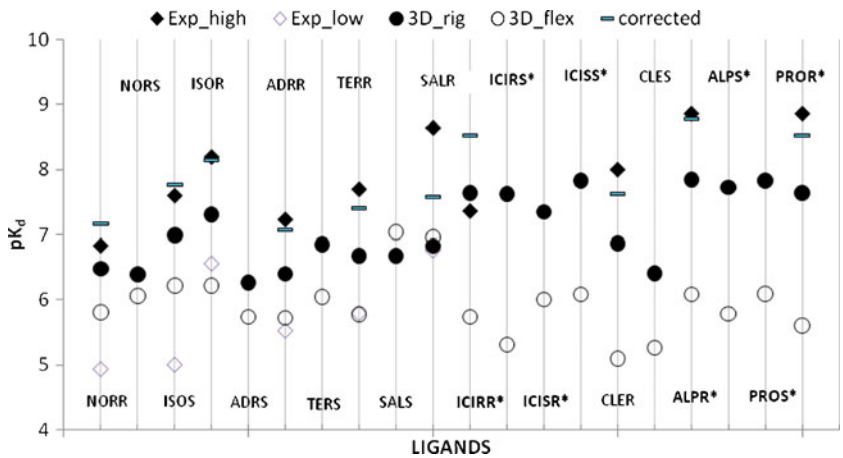

Fig. 5 Comparison between calculated and experimental (from Liang and Mills[18]) affinity values (pK_d) for the $p\beta_2AR$. Abbreviations: The first three letters correspond to those assigned each ligand in scheme 1 and the last to the isomeric form. Filled rhombs are high-affinity and open rhombs low-affinity pK_d values; black circles theoretical high-affinity pK_d values from the 3-D $p\beta_2AR$ refined model and blank circles are when the lateral chains of residues in TM5 are flexibles. Finally, hyphens are theoretical values corrected by the equation: Corrected value=1.2771(pK_d calculated)-1.0692, obtained from linear regression between experimental/theoretical values showed in supplementary Fig. 5. Asterisks are in antagonists or inverse agonists

values estimated from the flexible TM5-pβ_2AR were lower than those predicted in rigid pβ_2AR form (Fig. 5), and the gap between affinity predicted on site 1 and 2 increased, as evidenced by that fact that all the values for the second site were lower than the values observed in the rigid form.

For stereoisomer forms of salbutamol and ICI118,551, the predicted pK_d values are similar to those reported for racemates in experimental assays. Interestingly, the use of flexible lateral chains of residues in TM5 did improve the affinity prediction for ICI118,551on the pβ_2AR model, which could be a simple requirement for improving the described poor cross-dock of ICI118,551 on the hβ_2AR rigid crystal structures [59].

The affinity estimates for ICI118551 are uncharacteristically low for pβ_2AR (Table 2), compared with β_2ARs of other species, including human. We therefore suggest that the comparison of the pβ_2AR and hβ_2AR structural components that determine the affinity for ICI118,551 will provide rational starting points for the synthesis of chemical leads towards new receptor-selective β_2AR-blockers, which have potential clinical applications and currently are unavailable. Unlike for other ligands, affinity estimates for ICI118,551 in relation to native and recombinant hβ_2AR are approximately 20 times higher as well as being more reliable than those for pβ_2AR (Table 2), regardless of receptor density (yielding an average pK_B/pK_i~9.0).

To hypothetically account for this affinity difference, the binding partners for each of the four ICI118,551 stereoisomers were estimated on this pβ_2AR and on two refined hβ_2AR models (with/without flexible TM5 residues), one obtained by our workgroup and the other (with S-carazolol bound) kindly provided by V. Katritch [39, 40]. Similar

Table 2 Comparison of affinity estimates of ICI118,551 for porcine and human β_2-adrenoceptors. Data obtained from binding inhibition (pK_i), antagonism (pK_B) or by docking methodology

System	Receptor density (fmol.mg^{-1})	pβ_2AR		Receptor density (fmol.mg^{-1})	hβ_2AR	
		pK_i	pK_B		pK_i	pK_B
Experimental affinity						
Recombinant receptors expressed in CHO cells	–	7.4[18]		272	9.2[62]	
				466	9.3[63]	
Membranes from skeletal muscle	~50	6.4[64]				
Antagonism of uterus relaxation by isoprenaline and salbutamol	–		8.0			
			8.5[65]			
Antagonism of (-)adrenaline-evoked tachycardia	–		7.9[66]			
			7.7[66]			
Receptors expressed in murine heart				~4500	8.5[67]	
Ventricular receptors				~10	9.0[68]	
				–	8.9[69]	
Antagonism of ventricular adenylyl cyclase stimulation by (-)adrenaline				~10	8.9[70]	
Antagonism of atrial adenylyl cyclase stimulation by (-)adrenaline				~15	8.9[70]	
					9.1[71]	
Atrial receptors				~18	8.8[71]	
					9.2[69]	
Lung membranes				~33	8.9[72]	
Mast cell membranes				~9	8.9[72]	
Antagonism of histamine release from mast cells				~9		9.5[72]
Experimental AVERAGE		7.6			**9.0**	
Theoretical affinity[a]						
On Rigid model		7.83			6.72	
On flexible sidechains of TM5		6.08			8.92	

[a] The pKd values which represent the data of the high affinity S,S-ICI118,551- β_2AR complex in the binding site as described in this manuscript

hypothetical affinity values were found among isomers on both rigid porcine and rigid human β_2ARs. The flexibility of lateral chains of Tyr199, Ser203, Ser204 and Ser207 in TM5 yielded an increase in the estimated affinity value on hβ_2AR models and a decrease in the pβ_2AR (Suppl. Fig. 6). Unlike with the rigid hβ_2AR, the use of a flexible TM5 on the hβ_2AR resulted in an estimate of ICI118,551 affinity closely matching the affinity estimates reported from in vitro assays (Table 2).

We identified some different interactions of ICI118,551 on both the pβ_2AR and hβ_2AR models (Fig. 3) which could account for the differences in reported affinity values between these two β_2ARs. We therefore describe interactions of S,S-ICI118,551 with pk_d estimates and binding fit similar to those reported in the literature.

When S,S-ICI118,551 adopted a similar binding mode with the two β_2AR models (at the first site on hβ_2AR, Fig. 6:, S,S-ICI118,551 (pK_d=8.92; vdW+Hbond+desolv Energy=−8.18 kcal mol^{-1}, Electrostatic Energy=−0.61 kcal mol^{-1}, -moving ligand-moving receptor=−0.13) occupied a pocket formed by TM3 to TM7. When the ICI118,551 positions its aromatic ring toward TM5 and TM6 (with van der Walls -vdW-, hydrophobic or Π-Π interactions with Tyr199, Ser203, Ser204 and 207 in TM5, and Phe289, Phe290 and Asn293 in TM6 were predicted), its secondary amine group and its hydroxyl is in a crevice formed by Thr110, Ile112, Asp113 of TM3, Asn312 of TM7, and Phe193 at the top, and the isopropyl moiety is directed to the backbone segments of the amino acids Leu311, Asn312 and Tyr316 of TM7. In accordance with this finding, during the submission of this work, Wacker et al. published the ICI118,551-hβ_2AR complex with high similitude to our predicted site (Fig. 6) [59]. The RMSD between the crystallized and docked conformations of ICI118,551 ranks 0.49-2.28 for the greatest affinity complexes; being the major difference among these, the disposition of the ICI118,551 cyclic moieties. Also, carazolol, timolol and alprenolol showed a similar position when using this methodology on hβ_2AR, with the lowest RMSD between crystal and docked position being 0.43, 0.67 and 0.87, respectively.

Similarly on pβ_2AR, S,S-ICI118,551 (pK_d=7.83; vdW + Hbond + desolv Energy=−7.66 kcal mol^{-1}, Electrostatic Energy=−0.17 kcal mol^{-1}) was in a pocket formed by TM3 to TM6; ICI118,551 positions its aromatic group toward TM5 (having vdW and hydrophobic contacts with Tyr199, Ala200, Ser203 and Ser204 in this domain), at which time its secondary amine group and its hydroxyl is in a crevice formed by Ile110 and Asp113 of the TM3 and Phe193 at the top. Meanwhile, the isopropyl moiety is forward to a space limited by Val117 of TM3 and Trp286, Phe289 and Phe290 of TM6.

In alternative form, S,S-ICI118,551 docked (with similar affinity, pK_d=7.86; vdW + Hbond + desolv Energy=

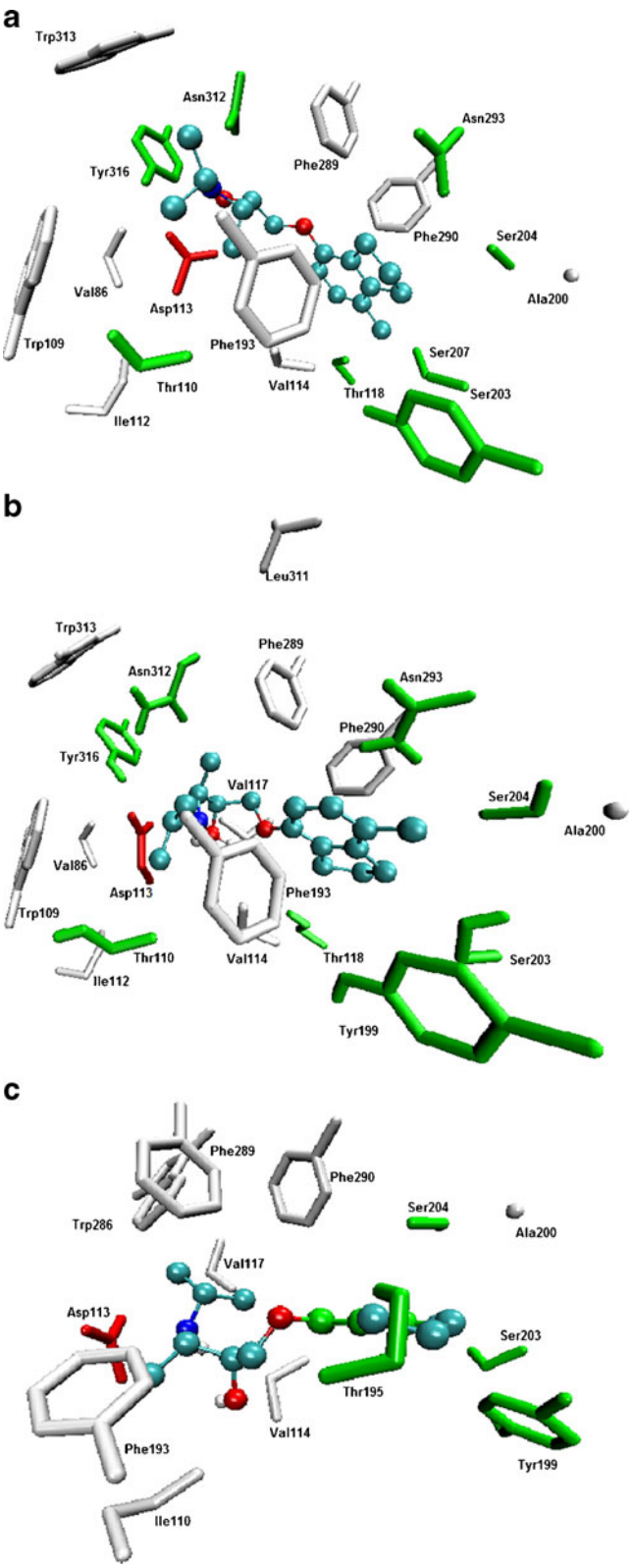

Fig. 6 The ligand S,S-ICI118,551 as is in the (**a**) crystal structure reported by Wacker et al. [59] and docked on the first site of flexibleTM5-hβ_2AR (**b**) and rigid-pβ_2AR (**c**). The side chains of amino acids reported as interacting residues from Autodock tools 1.5.0 are depicted accord the type of residue (see also Suppl. Fig. 4)

−7.08 kcal mol^{-1}, Electrostatic Energy=−0.78 kcal mol^{-1}) in the second binding site described for the majority of ligands on the pβ_2AR (Suppl. Fig. 4). In this case ICI118,551 positions its aromatic group into a crevice formed by TM6, TM7 and ECL2 (constituted by Asp192, Phe193, Phe289, His296, Lys305, Tyr308 and Ile309), its hydroxyl group is linked to the Asn312 and Tyr316 side chains by hydrogen bonds, and the secondary amine and isopropyl moieties are directed to the surface formed by Val86 and Gly90 of TM2 and the backbone of Trp109 of the TM3.

At the first site, our simulations suggest a greater number of contacts of ICI118,551with amino acids in the TM7 on the hβ_2AR than on the pβ_2AR (the amino acids are the same in this site for the β_2ARs of these two species). This greater number of contacts, together with the fact that the binding pocket in hβ_2AR appears be slightly greater than in pβ_2AR, can be implicated in the affinity differences between these two receptors. But this should be considered with caution due to the fact that with docking simulations only a conformational state of the β_2AR is analyzed, which can be improved by combining docking and molecular dynamics simulations.

The identification of essential amino acids in the ICI118,551-pβ_2AR complexes could be useful for future mutational studies under experimental methods. In brief, based on the visualizations described above, we can suggest that specific mutations in human (and/or porcine) β_2AR can disrupt the ICI118,551 binding. Thus, it can be expected that mutation of Thr110, Thr164 and Tyr174 (probably all together) for uncharged non-bulky side chain amino acids (like glycine) would reduce the volume of the binding pocket of hβ_2AR and consequently the number of possible interactions as well as the partial energies, thus decreasing the ICI118,551 affinity. Additionally, the mutation of Asn312, Tyr313 and Tyr316 (for glycine) could limit the binding participation of TM7-hβ_2AR. Conversely, substitution of Ile110 and/or Ile164 in pβ_2AR for an amino acid with polar uncharged side chain (threonine, serine, asparagine or glutamine) could modify the exposure of amino acids implicated in the ICI118,551-attachment on pβ_2AR, thus increasing the ICI118,551 affinity. Mutations in the residues included in the extracellular loops should also be tested due to their influence on the conformational disposition on transmembrane domains.

With regard to the stereoisomer forms, although R-enantiomers showed higher affinity than S-enantiomers in the majority of cases (at least 14 of 22 in each group of ligands-receptor simulations), no specific interactions with amino acids in the binding site were identified that could explain these differences.

Two affinity values have been found for agonists in pβ_2AR experiments [18]. In pβ_2AR expressed in Chinese hamster ovary cells, some agonists such as isoprenaline, adrenaline, noradrenaline, salbutamol, terbutaline and dobutamine exhibited GTP-dependent high- and low-affinity binding [18]. In our simulations, these ligands preferred binding site 1, judging by the affinity values corresponding to the two sites. However, two terbutyl-amine ligands, the partial agonists salbutamol and terbutaline, showed very similar affinity values for the two sites. For R or S terbutaline the affinity values were slightly greater on site 2, possibly as a result of the fact that terbutaline did not interact with Asp113 on the site 1 in this simulation, but maintained interaction with amino acids in TM5 (Ser203 and Ser204). It appears that site 1 is the high-affinity binding site for agonists, and that the affinity difference with site 2 can be important in biological systems if both sites are available in pβ_2AR. This is assumed to occur in an induced-agonist state due to the TM3-TM6 separation that is supported by experimental data [46], which would facilitate ligand entry.

In contrast, clenbuterol, zinterol, ractopamine, inverse agonists and antagonists all bound to a single site in the experimental assays with recombinant pβ_2AR [18]. Also, the hydrophilic ligand CGP12177, which has been shown to bind at two sites at hβ_1AR [48], apparently only bound to one site in hβ_2AR [60]. In these docking simulations it can be observed that clenbuterol and CGP12177 behave like other terbutyl-agonists (with similar affinity values at both sites), but with R-forms having a slight preference for site 1. This small difference could explain the experimental results consistent with the one-site model. Thus, these agonists could adapt to site 1 without inducing a conformational state in which the two sites would become available, possibly due to the lack of a catechol-like moiety in these ligands. In fact, CGP12177 has a similar moiety as other inverse agonists (see Fig. 1) and behaves as an antagonist on β_1AR at a high affinity site and as a partial agonist at a low affinity site [48]. Likewise, although antagonists and inverse agonists showed greater affinity for site 2 (Fig. 7), it is possible that most of the antagonists-induced conformational changes do not induce a state which exposes the two binding sites observed in our pβ_2AR model.

Possible implications of the second site found on the pβ_2AR model

In the current contribution theoretical evidence is provided by *docking* methods for the existence of two binding sites at the pβ_2AR, which is likely to exist for other 7TMs. Although in hβ_2AR only one site for CGP12177 has been identified, molecular dynamic studies have shown a separation of TM3 and TM6-TM7, which contain amino acids implicated in the micro-switches after ligand binding [42]. This fact increases the possibility of ligand accessibility to the binding site which we observed in our pβ_2AR 3-D model. Indeed, the conformational state of human

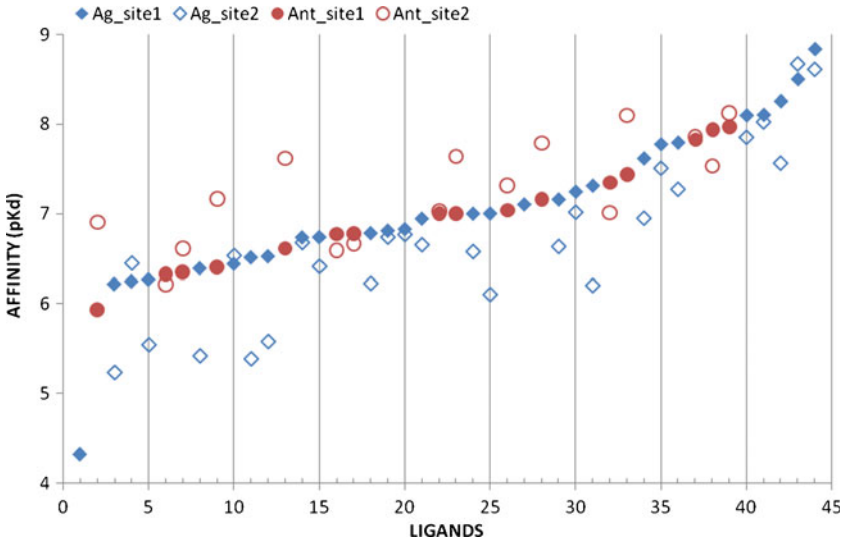

Fig. 7 Affinity values of ligands on the two binding sites identified on rigid form of $p\beta_2AR$. Antagonist or inverse agonist (circles) tend to high pK_d value on the second site, while agonist (rhombs) tend to high pK_d value on the first site. Values on the binding site 1 are filled symbols and on the binding site 2 empty symbols

β_2AR-adrenaline after 600 ns MD simulation shows the same two sites in similar dimensions as those found in our model (Suppl. Fig. 3).

Based on the aforementioned evidence, our model could represent a conformational state where the two binding sites become available for ligand binding. However, the existence of this state in nature could depend on the presence of a ligand on the receptor, which has been suggested for adrenaline, but not for noradrenaline, at $h\beta_2AR$ overexpressed in mouse heart [49]. The latter suggests that some moieties bound to the amine group of ligands could be necessary for the conformational state which exposes site 2. Additionally, the apparent ligand dependence to enter the low affinity binding site in β_2AR supports this possibility. The viability of this site for small ligands can be supported by the interaction of phenol ethylamine moiety of ZM241385 on a homologous site on the A_{2A} adenosine receptor [42]. Recently, mutations of amino acids in this receptor reveal the importance of homologous residues [61] to those identified in the $p\beta_2AR$ in the current contribution.

Finally, it should be mentioned that site 2 could be a ligand binding site which is exposed in a conformational state previous to the fit in the main site (site 1). This assumes that the first step in ligand recognition is the diffusion into the main site from the extracellular face of the β_2AR. In such a case, linkage to this site could modulate the conformation of ECL2 suggested as a partial lid for the funnel-like main binding site [42].

Conclusions

The present study aimed to determine an adequate molecular model of the 3-D structure for $p\beta_2AR$. Homology modeling and ab initio located in servers, as well as theoretical affinity studies by docking methods with well-known ligands were used to compare the similarities and differences between this model ($p\beta_2AR$) and $h\beta_2AR$ during the ligand recognition process. We selected a $p\beta_2AR$ 3-D model that was adequate for computational screening. In the $p\beta_2AR$ 3-D model, the ligands (agonists or antagonists) interacted in a similar form as found with $h\beta_2AR$. The experimental affinity data correspond to, or are close to those determined in this theoretical study. The docking procedure allowed us to study the similarities and differences in the recognition site(s) for ligands. In this sense, we focused at ICI118,551, since its lower affinity for $p\beta_2AR$ than $h\beta_2AR$ is well-known. The greater number of contacts with amino acids in the TM7 on the $h\beta_2AR$ than on the $p\beta_2AR$, together with the fact that the main binding pocket in $h\beta_2AR$ appears to be slightly more spacious than in $p\beta_2AR$ can be implicated in the higher affinity of ICI118,551 for the human receptor.

Although there is high similarity between $h\beta_2AR$ and $p\beta_2AR$, the few differences identified are revealing in terms of the possible differences in affinity to ligands. Thr110Ile, Thr164Ile, the different disposition on the Tyr174 residue and the volume of binding pocket formed by TM3 to TM7 appear to be essential differences between the main binding site 1 of these β_2ARs, implicating differences in contact between each of the ligands and $p\beta_2AR$. Additionally, a second binding site was identified on our $p\beta_2AR$ model. Some ligands -including ICI118,551- showed greater affinity on this site than for the other, consistent with observations in experimental assays.

In future studies, molecular dynamics simulations using this $p\beta_2AR$ model embedded in a lipid bilayer membrane could yield additional insights into the hypothesized binding sites and complexes, as well as to define the active/inactive states of the model and the identification of

key amino acids in specific ligand recognition and/or activation by specific ligands.

Acknowledgments We are grateful for the scholarships and financial support by the Consejo Nacional de Ciencia y Tecnología (Grant 62488), Comisión de Fomento de Actividades Académicas, y Secretaría de Investigación y Posgrado del Instituto Politécnico Nacional provided to MASU, JTF and JCB. Finally, we wish to thank Dr. Vsevolod Katritch for sharing the coordinates of his S-carazolol-hβ_2AR model for this study with us, and Bruce Allan Larsen for his critical reading of the manuscript. The hardware used in this study was purchased with INNOVAPyME program support (110703 and 139391) provided to Instituto Politécnico Nacional and Laboratorio Médico Químico Biológico.

References

1. Anderson GP (2006) Current issues with beta2-adrenoceptor agonists: pharmacology and molecular and cellular mechanisms. Clin Rev Allergy Immunol 31:119–130
2. Moody DE, Hancock DL, Anderson DB (2000) Phenetahnolamine repartitioning agents. In: D'Mello JPF (ed) Farma animal metabolism and nutrition. CAB International, Wallingford, pp 65–96
3. Rasmussen SG, Choi HJ, Rosenbaum DM, Kobilka TS, Thian FS, Edwards PC, Burghammer M, Ratnala VR, Sanishvili R, Fischetti RF, Schertler GF, Weis WI, Kobilka BK (2007) Crystal structure of the human beta2 adrenergic G-protein-coupled receptor. Nature 450:383–387
4. Cherezov V, Rosenbaum DM, Hanson MA, Rasmussen SG, Thian FS, Kobilka TS, Choi HJ, Kuhn P, Weis WI, Kobilka BK, Stevens RC (2007) High-resolution crystal structure of an engineered human beta2-adrenergic G protein-coupled receptor. Science 318:1258–1265
5. Hanson MA, Cherezov V, Griffith MT, Roth CB, Jaakola VP, Chien EY, Velasquez J, Kuhn P, Stevens RC (2008) A specific cholesterol binding site is established by the 2.8. A structure of the human beta2-adrenergic receptor. Structure 16:897–905
6. Rosenbaum DM, Cherezov V, Hanson MA, Rasmussen SG, Thian FS, Kobilka TS, Choi HJ, Yao XJ, Weis WI, Stevens RC, Kobilka BK (2007) 7TM engineering yields high-resolution structural insights into beta2-adrenergic receptor function. Science 318:1266–1273
7. Shukla AK, Sun J, Lefkowitz RJ (2008) Crystallizing thinking about the β2-adrenergic receptor. Mol Pharmacol 73:1333–1338
8. Costanzi S (2008) On the applicability of 7TM models to computer-aided drug discovery: a comparison between in silico and crystal structure of the β2-adrenergic receptor. J Med Chem 51:2907–2914
9. Topiol S, Sabio M (2008) Use of the X-ray structure of the Beta2-adrenergic receptor for drug discovery. Bioorg Med Chem Lett 18:1598–1602
10. De Graaf C, Rognan D (2008) Selective structure-based virtual screening for full and partial agonist of the β2 adrenergic receptor. J Med Chem 51:4978–4985
11. Hausch F (2008) Betablockers at work: the crystal structure of the beta2-adrenergic receptor. Angew Chem Int Ed Engl 47:3314–3316
12. Canning BJ, Chou Y (2008) Using guinea pigs in studies relevant to asthma and COPD. Pulm Pharmacol Ther 21:702–720
13. Soriano-Ursúa MA, Trujillo-Ferrara J, Correa-Basurto J (2009) Homology modeling and flex-ligand docking studies on the guinea pig β2 adrenoceptor: structural and experimental similarities/ differences with the human β2. J Mol Model 15:1203–1211
14. Mustafi D, Palczewski K (2009) Topology of class A G protein-coupled receptors: insights gained from crystal structures of rhodopsins, adrenergic and adenosine receptors. Mol Pharmacol 75:1–12
15. Fatakia SN, Costanzi S, Chow CC (2009) Computing highly correlated positions using mutual information and graph theory for G protein-coupled receptors. PLoS ONE 4:e4681
16. Römpler H, Stäubert C, Thor D, Schulz A, Hofreiter M, Schöneberg TG (2007) Protein-coupled time travel: evolutionary aspects of 7TM research. Mol Interv 7:17–25
17. Burgisser E, Hancock AA, Lefkowitz RJ, Delean A (1981) Anomalous equilibrium binding properties of high-affinity racemic radioligands. Mol Pharmacol 19:205–216
18. Liang W, Mills S (2001) Profile of ligand binding to the porcine β2 adrenergic receptor. J Anim Sci 79:877–883
19. Soriano-Ursúa MA, Trujillo-Ferrara JG, Correa-Basurto J (2010) Scope and difficulty in generating theoretical insights regarding ligand recognition and activation of the beta 2 adrenergic receptor. J Med Chem 53:923–932
20. Liang W, Bidwell CA, Williams SK, Mills SE (1997) Rapid communication: molecular cloning of the porcine beta 2-adrenergic receptor gene. J Anim Sci 75:2824
21. Zhang Y (2008) I-TASSER server for protein 3D structure prediction. BMC Bioinform 9:40
22. Zhang Y (2007) Template-based modeling and free modeling by I-TASSER in CASP7. Proteins 8:108–117
23. Wu S, Skolnick J, Zhang Y (2007) Ab initio modeling of small proteins by iterative TASSER simulations. BMC Biol 5:17
24. Arnold K, Bordoli L, Kopp J, Schwede T (2006) The Swiss-model workspace: a web-based environment for protein structure homology modeling. Bioinformatics 22:195–201
25. Schwede T, Kopp J, Guex N, Peitsch MC (2003) Swiss-model: an automated protein homology-modeling server. Nucleic Acids Res 31:3381–3385
26. Guex N, Peitsch MC (1997) Swiss-model and the Swiss-PdbViewer: an environment for comparative protein modeling. Electrophoresis 18:2714–2723
27. Chen CC, Hwang JK, Yang JM (2006) $(PS)^2$: protein structure prediction server. Nucleic Acids Res 34:W152–W157
28. Kobilka BK (2007) G protein coupled receptor structure and activation. Biochim Biophys Acta 1768:794–807
29. Zhang Y, Skolnick J (2004) Scoring function for automated assessment of protein structure template quality. Proteins 57:702–710
30. Lovell SC, Davis IW, Arendall WB 3rd, de Bakker PI, Word JM, Prisant MG, Richardson JS, Richardson DC (2003) Structure validation by Calpha geometry: phi, psi and Cbeta deviation. Proteins 50:437–450
31. Phillips JC, Braun R, Wang W, Gumbart J, Tajkhorshid E, Villa E, Chipot C, Skeel RD, Kale L, Schulten K (2005) Scalable molecular dynamics with NAMD. J Comput Chem 26:1781–1802
32. Zhang Y, Skolnick J (2005) TM-align: a protein structure alignment algorithm based on the TM-score. Nucleic Acids Res 33:2302–2309
33. Soriano-Ursúa MA, Valencia-Hernández I, Arellano-Mendoza MG, Correa-Basurto J, Trujillo-Ferrara JG (2009) Synthesis, pharmacological and in silico evaluation of 1-(4-di-hydroxy-3, 5-dioxa-4-borabicyclo[4.4.0]deca-7, 9, 11-trien-9-yl)-2-(tert-butyl-amino) etha-nol, a compound designed to act as a β2 adreno-ceptor agonist. Eur J Med Chem 44:2840–2846
34. Frisch MJ, Trucks GW, Schlegel HB et al (1998) Gaussian 98, Version A.7. Gaussian Inc, Pittsburgh, PA
35. Laurie AT, Jackson RM (2005) Q-SiteFinder: an energy-based method for the prediction of protein-ligand binding sites. Bioinformatics 21:1908–1916
36. Morris GM, Goodsell DS, Halliday RS, Huey R, Hart E, Belew RK, Olson JA (1998) Automated docking using a Lamarckian genetic algorithm and empirical binding free energy function. J Comput Chem 19:1639–1662

37. Goodford PJ (1985) A computational procedure for determining energetically favorable binding sites on biologically important macromolecules. J Med Chem 28:849–857
38. Humphrey W, Dalke A, Schulten K (1996) VMD: visual molecular dynamics. J Mol Graph 14:33–38
39. Katritch V, Reynolds KA, Cherezov V, Hanson MA, Roth CB, Yeager M, Abagyan R (2009) Analysis of full and partial agonists binding to beta2-adrenergic receptor suggests a role of transmembrane helix V in agonist-specific conformational changes. J Mol Recognit 22:307–318
40. Soriano-Ursúa MA, Trujillo-Ferrara JG, Correa-Basurto J (2010) Docking studies on a refined human β_2 adrenoceptor model yield theoretical affinity values in function with experimental values for R-ligands, but not for S-antagonists. J Mol Model 16:401–409
41. Audet M, Bouvier M (2008) Insights into signaling from the beta2-adrenergic receptor structure. Nat Chem Biol 4:397–403
42. Nygaard R, Frimurer TM, Holst B, Rosenkilde MM, Schwartz TW (2009) Ligand binding and micro-switches in 7TM receptor structures. Trends Pharmacol Sci 30:249–259
43. Green SA, Rathz DA, Schuster AJ, Liggett SB (2001) The Ile164 beta(2)-adrenoceptor polymorphism alters salmeterol exosite binding and conventional agonist coupling to G(s). Eur J Pharmacol 421:141–147
44. Green SA, Cole G, Jacinto M, Innis M, Liggett SB (1993) A polymorphism of the human beta 2-adrenergic receptor within the fourth transmembrane domain alters ligand binding and functional properties of the receptor. J Biol Chem 268:23116–23121
45. Swaminath G, Deupi X, Lee TW, Zhu W, Thian FS, Kobilka TS, Kobilka B (2005) Probing the β_2 adrenoceptor binding site with catechol reveals differences in binding and activation by agonist and partial agonists. J Biol Chem 280:22165–22171
46. Bokoch MP, Zou Y, Rasmussen SG, Liu CW, Nygaard R, Rosenbaum DM, Fung JJ, Choi HJ, Thian FS, Kobilka TS, Puglisi JD, Weis WI, Pardo L, Prosser RS, Mueller L, Kobilka BK (2010) Ligand-specific regulation of the extracellular surface of a G-protein-coupled receptor. Nature 463:108–112
47. Kobilka BK, Deupi X (2007) Conformational complexity of G-protein-coupled receptors. Trends Pharmacol Sci 28:397–406
48. Kaumann AJ, Molenaar P (2008) The low-affinity site of the beta1-adrenoceptor and its relevance to cardiovascular pharmacology. Pharmacol Ther 118:303–336
49. Heubach JF, Ravens U, Kaumann AJ (2004) Epinephrine activates both Gs and Gi pathways, but norepinephrine activates only the Gs pathway through human beta2-adrenoceptors overexpressed in mouse heart. Mol Pharmacol 65:1313–1322
50. Battacharya S, Hall SE, Li H, Vaidehi N (2008) Ligand stabilized conformational states of human beta 2 adrenergic receptor: insight into G protein coupled receptor activation. Biophys J 94:2027–2042
51. Rubenstein LA, Zauhar RJ, Lanzara RG (2006) Molecular dynamics of a biophysical model for beta2-adrenergic and G protein-coupled receptor activation. J Mol Graph Model 25:396–409
52. Dror RO, Arlow DH, Borhani DW, Jensen MØ, Piana S, Shaw DE (2009) Identification of two distinct inactive conformations of the beta2-adrenergic receptor reconciles structural and biochemical observations. Proc Natl Acad Sci USA 106:4689–4694
53. Huber T, Menon S, Sakmar TP (2009) Structural basis for ligand binding and specificity in adrenergic receptors: implications for 7TM-targeted drug discovery. Biochemistry 47:11013–11023
54. Rosenbaum DM, Rasmussen SG, Kobilka BK (2009) The structure and function of G-protein-coupled receptors. Nature 459:356–363
55. Galandrin S, Bouvier M (2006) Distinct signaling profiles of β1 and β2 adrenergic receptor ligands towards adenylyl cyclase and mitogen-activated protein kinase reveals the pluridimensionality of efficacy. Mol Pharmacol 70:1575–1584
56. Jaakola VP, Griffith MT, Hanson MA, Cherezov V, Chien EY, Lane JR, Ijzerman AP, Stevens RC (2008) The 2.6 angstrom crystal structure of a human A2A adenosine receptor bound to an antagonist. Science 322:1211–1217
57. Chelikani P, Hornak V, Eilers M, Reeves PJ, Smith SO, RajBhandary UL, Khorana HG (2007) Role of group-conserved residues in the helical core of beta2-adrenergic receptor. Proc Natl Acad Sci USA 104:7027–7032
58. Fraser CM (1989) Site-directed mutagenesis of β-Adrenergic receptor. J Biol Chem 264:9266–9270
59. Wacker D, Fenalti G, Brown MA, Katritch V, Abagyan R, Cherezov V, Stevens RC (2010) Conserved binding mode of human β2 adrenergic receptor inverse agonists and antagonist revealed by X-ray crystallography. J Am Chem Soc 132:11443–11445
60. Baker JG, Hall IP, Hill SJ (2002) Pharmacological characterization of CGP12177 at the human beta(2) adrenoceptor. Br J Pharmacol 137:400–408
61. Jaakola VP, Lane JR, Lin JY, Katritch V, Ijzerman AP, Stevens RC (2010) Ligand binding and subtype selectivity of the human A (2A) adenosine receptor: identification and characterization of essential amino acid residues. J Biol Chem 285:13032–13044
62. Hoffmann C, Leitz MR, Oberdorg-Maass S, Lohse MJ, Klotz KN (2004) Comparative pharmacology of human β-adrenergic receptor subtypes – characterization of stably transfected in CHO cells. Naunyn Schmiedebergs Arch Pharmacol 369:151–159
63. Baker JG (2005) The selectivity of β-adrenoceptor antagonists at the human β1-, β2- and β3-adrenoceptors. Br J Pharmacol 144:317–322
64. Sillence MN, Hooper J, Zhou GH, Liu Q, Munn KJ (2005) Characterization of porcine beta1- and beta2-adrenergic receptors in heart, skeletal muscle, and adipose tissue, and the identification of an atypical beta-adrenergic binding site. J Anim Sci 83:2339–2348
65. Yamanishi T, Chapple CR, Yasuda K, Yoshida K, Chess-Williams R (2003) The functional role of beta-adrenoceptor subtypes in mediating relaxation of pig urethral smooth muscle. J Urol 170:2508–2511
66. Galindo-Tovar A, Vargas ML, Kaumann AJ (2010) Function of cardiac β_1- and β_2-adrenoceptors of newborn piglets: role of phosphodiesterases PDE3 and PDE4. Eur J Pharmacol 638:99–107
67. Heubach JF, Trebeb T, Wettwer E, Himmel HM, Michel MC, Kaumann AJ, Koch WJ, Harding SE, Ravens U (1999) L-type Ca^{2+} current and contractility in ventricular myocytes from mice overexpressing the cardiac β_2-adrenoceptor. Cardiovasc Res 42:173–182
68. Kaumann AJ, Lemoine H (1987) β_2-adrenoceptor-mediated positive inotropic effects of adrenaline in human ventricular myocardium. Quantitative discrepancies with binding and adenylate cyclase stimulation. Naunyn Schmiedebergs Arch Pharmacol 335:403–411
69. Buxton BF, Jones CR, Molenaar P, Summers RJ (1987) Characterization and autoradiographic localization of beta-adrenoceptor subtypes in human cardiac tissues. Br J Pharmacol 92:299–310
70. Gille E, Lemoine H, Ehle B, Kaumann AJ (1985) The affinity of (-)-propanolol for β_1- and β_2-adrenoceptors of human heart. Differential antagonism of the positive inotropic effects and adenylate cyclase stimulation by (-)-noradrenaline and (-)-adrenaline. Naunyn Schmiedebergs Arch Pharmacol 331:60–70
71. Lemoine H, Schönell H, Kaumann AJ (1988) Contribution of β_1- and β_2-adrenoceptors of human atrium and ventricle to the effects of noradrenaline and adrenaline as assessed with (-)-atenolol. Br J Pharmacol 95:55–66
72. Chong JK, Chess-Williams R, Peachell PT (2002) Pharmacological characterization of the β-adrenoceptor expressed by human mast cells. Eur J Pharmacol 437:1–7